ORIGINAL PAPER

The synthesis of Cu(II), Zn(II), and Co(II) metalloporphyrins and their improvement to the property of Li/SOCl₂ battery

Zengqi Zhang · Luyao Kong; · Ying Xiong · Yun Luo ·
Jun Li

Abstract One new porphyrin, 5,10,15-triphenyl-20-[4-(2-(4-formoxyl)phenoxy)ethoxy]phenyl porphyrin, and its three corresponding copper(II), cobalt(II), and zinc (II) complexes were synthesized and characterized by IR, UV–vis, ^{1}H NMR, MS, and elementary analysis. Their improvements to the lithium/thionyl chloride (Li/SOCl₂) battery were also tested. The results show that the discharge time of Li/SOCl₂ battery with porphyrin/metalloporphyrins is approximately 502–692 s longer than that of Li/SOCl₂ battery in blank. The maximum initial discharge voltage of battery with the existence of metalloporphyrins is also increased. The energy of Li/SOCl₂ battery in blank is 96.3 J while that of Li/SOCl₂ battery after adding porphyrin/metalloporphyrins is 153.1 J for metal-free porphyrin, 133.6 J for Cu(II) porphyrin, 167.2 J for Co(II) porphyrin, and 158.3 J for Zn(II) porphyrin, respectively. With increasing battery discharge time by 691.3 s and enhancing maximum discharge voltage by 0.04 V, the Co(II) porphyrin exhibits the best improvement to Li/SOCl₂ battery. The results of cyclic voltammetry show that the adding of porphyrins improves the reduction rate of SOCl₂.

Keywords Porphyrin · Metalloporphyrin · Synthesis · Improvement · Li/SOCl₂ battery

Introduction

The development of high-performance primary batteries is one of the most important research subjects due to the ever-increasing energy demands and pressing environmental concerns [1–6]. Lithium/thionyl chloride (Li/SOCl₂) battery, which is high energy density, high operation voltage, long storage life, and wide operation temperature range (−55~85 °C), has been widely used to power various electronic devices for industrial and military applications [7, 8]. However, in practice, the energy of Li/SOCl₂ battery is much lower than that in theory, which severely prevents its extensive application [6, 9]. This is mainly because deposition of LiCl clogged the porous carbon cathode [10, 11]. To overcome these problems, some catalysts which are able to improve the discharge capability of the Li/SOCl₂ battery have been developed. Among these catalysts, some macromolecular compounds, such as metal phthalocyanine derivatives, have attracted considerable interest [12, 13]. Due to its high conjugated structure, good thermal stability, excellent electron conductivity, and better solubility, metal phthalocyanines can improve the performance of Li/SOCl₂ battery [14, 15].

As we all know, porphyrin derivatives have similar structure to phthalocyanine derivatives and exhibit good thermal stability and excellent catalytic, optical, and electrical properties [16–23]; therefore, the porphyrin derivatives are applied to Li/SOCl₂ battery system to improve its discharge voltage and battery energy. Nevertheless, to the best of our knowledge, only few works have demonstrated the improvement activity of metalloporphyrins to Li/SOCl₂ battery [24–27]. Here, we report the synthesis, characterization of one metal-free porphyrin, and its three metalloporphyrin complexes, shown in Fig. 1, and studied their enhancement to Li/SOCl₂ battery.

Experimental

Materials and reagents

LiAlCl₄/SOCl₂ electrolyte (the concentration of LiAlCl₄ is 1.47 M), lithium pieces, and carbon films were provided by

Z. Zhang · L. Kong; · Y. Xiong · Y. Luo · J. Li (✉)
Key Laboratory of Synthetic and Natural Functional Molecule
Chemistry of Ministry of Education, College of Chemistry and
Materials Science, Northwest University, Xi'an, Shaanxi 710069,
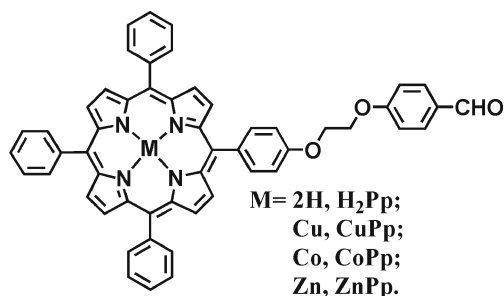People's Republic of China
e-mail: junli@nwu.edu.cn

Fig. 1 The chemical structures of porphyrin complexes

Xi'an Institute of Electromechanical Information Technology. 4-Hydroxybenzaldehyde and 4-(2-bromoethoxy)benzaldehyde were obtained from Sinopharm Chemical Reagent Co. Ltd., and other reagents were purchased from Tianjin Chemical Reagents Company. They were used directly except pyrrole which was distilled before use.

Equipment

^{1}H NMR spectra were recorded by means of a Varian Inova 400-MHz apparatus at room temperature; CDCl$_3$ was employed as solvent and tetramethylsilane (TMS) for reference. Elemental analyses (C, H, and N) were performed by Vario EL-III CHNOS instrument. Fourier transform infrared (FT-IR) spectra were obtained with samples in KBr pellets on a BEQUZNDX-550 spectrometer. Mass spectrometry (MS) analyses were carried out on a matrix-assisted laser desorption/ionization time of flight mass spectrometer (MALDI-TOF MS, Krato Analytical Company of Shimadzu Biotech, Manchester, Britain). UV–vis spectra were measured on a Shimadzu UV1800 UV–vis–NIR spectrophotometer.

Synthesis

The synthetic routes to the porphyrin and metalloporphyrins are shown in Scheme 1. The detailed synthetic procedures are as follows:

5-(4-Hydroxyphenyl)-10,15,20-triphenylporphyrin

According to the method previously reported [28], the 5-(4-hydroxyphenyl)-10,15,20-triphenylporphyrin was synthesized by 4-hydroxybenzaldehyde (15 mmol, 1.83 g) and benzaldehyde (45 mmol, 4.6 mL) and pyrrole (60 mmol, 4.15 mL) reacted in refluxing propionic acid for about 50 min. When the reaction was finished, the crude product was acquired and it was purified on a silica gel column with dichloromethane as eluent. Yield: 25 %. Mp: >250 °C. Anal. calcd. (found) for C$_{44}$H$_{30}$N$_4$O (mol. wt: 630.74), %: C, 83.75 (83.79); H, 4.78 (4.79); N, 8.91 (8.88). MS: *m/z* 631.2 ([M+H]$^+$) amu. UV–vis (CH$_2$Cl$_2$): λ_{max}/nm, 420 (Soret band) and 517, 550, 590, and 654 (Q

bands). FT-IR: υ, cm^{-1}, 3,429, 3,316, 3,053, 1,610, 1,472, 1,349, 1,217, 1,073, 966, 800, and 702.

5,10,15-triphenyl-20-[4-(2-(4-formoxyl)phenoxy)ethoxy] phenyl porphyrin (H$_2$Pp)

The 5-(4-hydroxyphenyl)-10,15,20-triphenylporphyrin (0.2 mmol, 0.126 g) and 4- (2-bromoethoxy) benzaldehyde (2 mmol, 0.458 g) were dissolved in 10 mL of N,N-dimethylformamide (DMF). Then the solution was stirred in the presence of K$_2$CO$_3$ for 12 h at 60 °C in the darkness. The DMF was evaporated under vacuum after completing the reaction, and the residue was dissolved in CH$_2$Cl$_2$ and purified on a silica gel column using dichloromethane as eluent. Yield: 85 %. Mp: >250 °C. Anal. calcd. (found) for C$_{53}$H$_{38}$N$_4$O$_3$ (mol. wt: 778.89), %: C, 81.71 (81.73); H, 4.96 (4.92); N, 7.21 (7.19). MS: *m/z* 779.71 ([M+H]$^+$) amu. UV–vis (CH$_2$Cl$_2$): λ_{max}/nm, 415 (Soret band) and 511, 554, 588, and 651 (Q bands). FT-IR: υ, cm^{-1}, 3,419, 2,797, 2,734, 1,687, 1,601, 1,577, 1,507, 1,253, 965, 830, and 800. ^{1}H NMR (CDCl$_3$, 400 MHz): δ, ppm 9.90 (s, 1H, aldehyde-H), 8.85 (m, 8H, β position of the pyrrole moiety), 8.22 (m, 6H, ortho-phenyl-H), 7.84 (m, 9H, meta- and paraphenyl-H), 7.75–7.20 (d, d, 4H, substituted phenyl-H), 5.28 (m, 4H, phenyl-H), 4.42, 3.61 (t, t, 2H, 2H, CH$_2$-CH$_2$), and −2.76 (s, 2H, imino-H).

General procedure for the synthesis of MPp (M=Cu^{2+}, Co^{2+}, Zn^{2+})

0.5 mmol of M(NO$_3$)$_2$ (M=Cu^{2+}, Co^{2+}, Zn^{2+}) and 0.05 mmol of H$_2$Pp were dissolved in 20 mL dichloromethane and 5 mL ethanol. And then the mixture solution was stirred at room temperature for 12 h and monitored by TLC until the H$_2$Pp disappeared. The unreacted solid salt was filtered, and the solvent was removed under vacuum. The crude was purified on a silica gel column with dichloromethane as eluent.

CuPp. Yield: 95 %. Mp: >250 °C. Anal. calcd. (found) for C$_{53}$H$_{36}$N$_4$O$_3$Cu (mol. wt: 840.42), %: C, 75.78 (75.74); H, 4.30 (4.32); N, 6.65 (6.67). MS: *m/z* 841.71 ([M+H]$^+$) amu. UV–vis (CH$_2$Cl$_2$): λ_{max}/nm, 414 (Soret band) and 538 and 574 (Q bands). FT-IR: υ, cm^{-1}, 3,437, 2,925, 2,803, 2,730, 1,685, 1,601, 1,504, 1,251, 1,161, 1,002, and 827.

CoPp. Yield: 50 %. Mp: >250 °C. Anal. calcd. (found) for C$_{53}$H$_{36}$N$_4$O$_3$Co (mol. wt: 835.81), %: C, 76.78 (76.16); H, 4.30 (4.34); N, 6.67 (6.70). MS: *m/z* 836.90 ([M+H]$^+$) amu. UV–vis (CH$_2$Cl$_2$): λ_{max}/nm, 414 (Soret band) and 529 (Q bands). FT-IR: υ, cm^{-1}, 3,437, 2,839, 2,742, 1,688, 1,600, 1,257, 1,156, 1,009, and 802.

ZnPp. Yield: 85 %. Mp: >250 °C. Anal. calcd. (found) for C$_{53}$H$_{36}$N$_4$O$_3$Zn (mol. wt: 842.27), %: C, 75.68 (75.58); H, 4.30 (4.31); N, 6.66 (6.65). MS: *m/z* 843.54 ([M+H]$^+$) amu. UV–vis (CH$_2$Cl$_2$): λ_{max}/nm, 417 (Soret band) and 545 and 623 (Q bands). FT-IR: υ, cm^{-1}, 3,440, 2,853, 2,736, 1,668, 1,598, 1,265, 1,161, 999, and 798.

Scheme 1 Syntheses of the
porphyrin and metalloporphyrins
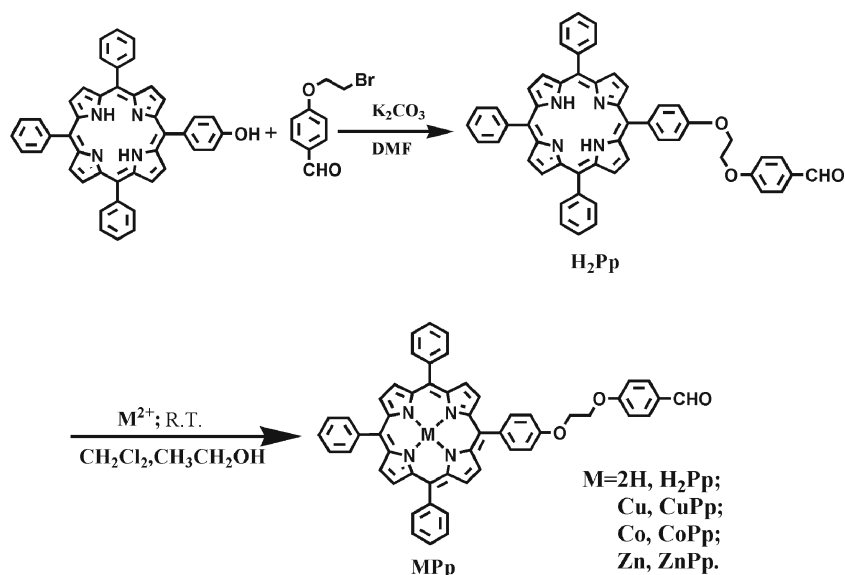
Electrochemical measurements

The electrochemical measurement of Li/SOCl₂ battery was accomplished in specially designed test cells [29], shown in Fig. 2. The compartment of the cells is made from polytetrafluoroethylene (PTFE) material. Carbon films were used as cathode with the apparent area of 1 cm², and the clean lithium pieces were employed as the counter electrodes. All the materials and reagents were dried in vacuum at 70°C for 4 h before use. One milliliter LiAlCl₄/SOCl₂ electrolyte solution contains 2 mg MPp (M=2H, Cu, Zn, Co). The discharge tests for the Li/SOCl₂ batteries are evaluated at ambient temperature 25 °C, constant resistance of 40Ω. The Li/SOCl₂ battery is assembled in dry room facility, in which the relative humidity is kept below 1 %. In the progress, the output voltage (U) of the battery is measured with time until the battery continuously discharging to 2 V.

Fig. 2 The Li/SOCl₂ battery

Cyclic voltammetry

The cyclic voltammetry was conducted with a scan rate of 100 mV s^{-1}. Before measurement of CV began, the electrodes were polarized at least 3 min at 5 V to eliminate the LiCl film formed on the electrode surface. The *i–E* curves were recorded by a CHI660 electrochemical workstation.

Results and discussion

Synthesis of the porphyrin and metalloporphyrins

The synthetic routes of porphyrin (H₂Pp) and metalloporphyrins (CuPp, CoPp, ZnPp) were illustrated in Scheme 1.

The 5-(4-hydroxyphenyl)-10,15,20-triphenylporphyrin was obtained by benzaldehyde, 4-hydroxybenzaldehyde, and pyrrole reacting in propionic acid. The porphyrin H₂Pp was synthesized by treating 5-(4-hydroxyphenyl)-10,15,20-triphenylporphyrin and 4-(2-bromoethoxy)benzaldehyde in DMF with the presence of K₂CO₃. The metalloporphyrins were obtained by the reaction of H₂Pp with an excess of M(NO₃)₂ (M=Cu²⁺, Co²⁺, Zn²⁺) in the mixed solvents CH₂Cl₂ and C₂H₅OH.

Spectral characterization of the porphyrin and metalloporphyrins

The UV–vis spectrum of H₂Pp shows a Soret band at 415 nm and four Q bands at 510, 554, 592, and 651 nm, while for CuPp, CoPp, and ZnPp, the UV–vis spectra exhibit one Soret

band at 415 nm and one/two Q bands (538–550 and 572–590 nm). The decreased number of Q bands in the metalloporphyrin complexes is due to the symmetry increase of porphyrin ring when the metal ions coordinate with the N atoms of porphyrin (Fig. 3). The delocalized π bonds decrease the average electron density in the metalloporphyrins which increased the energy available for electron transition as a result, a blue shift of the Soret bands occurred in these metalloporphyrins.

In the FT-IR spectroscopy data (Table 1), the absorption peaks around 3,419–3,440 cm^{-1} and 960–965 cm^{-1}, observed in H$_2$Pp, are related to the stretching and bending vibration of the central porphyrin N-H [30–32], and as expected, these peaks are absent from the spectra of MPp in which four N atoms coordinate with metal ion. The band around 1,680 cm^{-1}, found in the spectra of both H$_2$Pp and MPp, is associated with stretching vibrations of C=O; and the band at 1,250 cm^{-1} is attributed to the stretching vibrations of C-O. The stretching vibrations of C-H around 2,800 cm^{-1} can be observed.

The ^{1}H NMR spectrum of H$_2$Pp is consistent with its molecular structure. The aldehyde proton chemical shift is 9.90 ppm. The chemical shift of protons in β position of porphyrin is around 8.84 ppm, and that of phenyl protons is observed in the range of 7.25–8.22 ppm. The chemical shift of protons in two CH$_2$ groups is at 4.61 ppm while that of NH groups at −2.77 ppm.

Crystal structure of CuPp

The single crystal of CuPp was obtained by the evaporation of CH$_2$Cl$_2$ solvent slowly. The single crystal X-ray diffraction analysis reveals that CuPp crystallizes in triclinic P-1 space group. As shown in Fig. 4a, The Cu^{2+} ion coordinates to four N atoms with the Cu-N distances in the range from 1.974 to
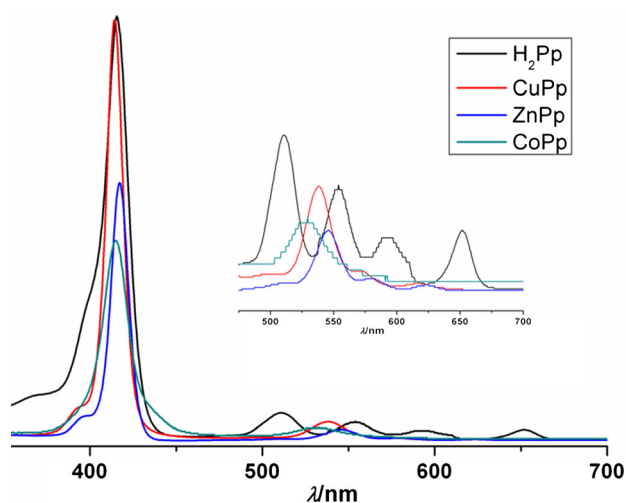
Table 1 Mass spectroscopy and FT-IR spectroscopy of porphyrins

Porphyrin	MS (m/z, [M+1]$^+$)	FT-IR (v, cm^{-1})
H$_2$Pp	779.71	3,419 (v_{NH}), 1,687 ($v_{C=O}$), 1,253 (v_{C-O-Ph}), 965 (δ_{NH})
CuPp	841.71	1,685 ($v_{C=O}$), 1,251 (v_{C-O-Ph})
CoPp	836.90	1,688 ($v_{C=O}$), 1,257 (v_{C-O-Ph})
ZnPp	843.54	1,668 ($v_{C=O}$), 1,265 (v_{C-O-Ph})

1.997 Å. The twist angles between the peripheral phenyl rings and porphyrin plane is 60.995–75.956°. The 3D supramolecular structure (Fig. 4b, c) can be formed taking into account π-π staking, in which the porphyrin macrocycles are parallel to each other.

Electrochemical property of Li/SOCl$_2$ battery

Figure 5 shows the typical discharge curves measured on the pure carbon electrode. It can be readily seen that the performance of Li/SOCl$_2$ battery with the presence of porphyrin complexes is better than that of Li/SOCl$_2$ battery in the absence of the porphyrins. The battery discharge time above 2 V is 1,791.2 s for H$_2$Pp, 1,675.8 s for CuPp, 1,865.1 s for CoPp, and 1,730.4 s for ZnPp, respectively, while that in the absence of porphyrins is only 1,173.8 s. Moreover, compared with the blank, the maximum initial discharge voltage of battery enhanced 0.01, 0.04, and 0.03 V in the presence of H$_2$Pp, CoPp, and ZnPp, respectively, and only a decreased initial discharge voltage with the CuPp. Particularly, with increasing battery discharge time by 691.3 s and enhancing maximum discharge voltage by 0.04 V, the CoPp shows highest improvement to Li/SOCl$_2$ battery.

In order to explain the improvement of the compounds to Li/SOCl$_2$ battery, the relative energy of Li/SOCl$_2$ battery was calculated as follows:

The average discharge voltage of Li/SOCl$_2$ battery is

$$U_{av} = \frac{\sum U \Delta t}{\sum \Delta t}$$
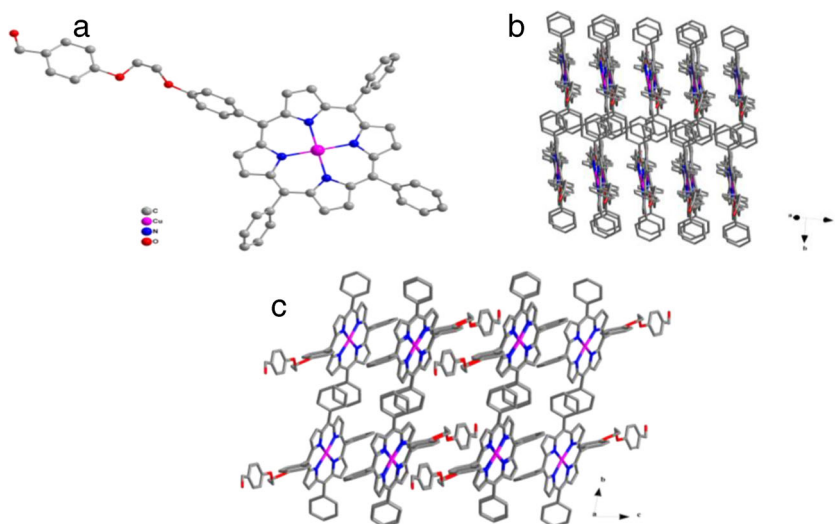
The energy of Li/SOCl$_2$ battery is

$$E = \int pdt = \frac{1}{R_e} \sum U^2 \Delta t$$

The capacity of Li/SOCl$_2$ battery is

$$C = \int Idt = \int {U}/{R_e} dt = \frac{1}{R_e} \sum U \Delta t$$

In which U stands for the discharge voltage, t stands for the discharged time, U_{av} stands for the average discharge voltage

Fig. 3 UV–vis spectra of porphyrins

Fig. 4 **a** The coordination environment of the Cu(II) ion, **b** illustration of the CuPp array, and **c** view of the crystal structure down the a axis

of the battery, E stands for the energy of the battery, C stands for the capacity of the battery. P stands for the power of the battery, and R_e stands for the external resistance.

The energy of Li/SOCl$_2$ battery reflects the enhancement of porphyrins clearly (shown in Table 2). It shows that the energy of Li/SOCl$_2$ battery with H$_2$Pp, CuPp, CoPp, and ZnPp is 153.1, 133.6, 167.2, and 158.3 J, respectively, higher than that of Li/SOCl$_2$ battery in the absence of porphyrins, which is only 96.3 J, (shown in Fig. 6). It can be easily seen that CoPp shows the most effective improvement for Li/SOCl$_2$ battery. The capacity of battery with porphyrins is in range from 13.1 to 15.5 mA h, higher than that of battery in absence of porphyrins (9.3 mA h).

The cyclic voltammetry of Li/SOCl$_2$ batteries in the presence of porphyrin or metalloporphyrins was tested. As shown in Fig. 7, there are two reduction peaks, which correspond to

the reduction of SOCl$_2$, and the corresponding oxidation peaks are negligible. This indicates that the reduction of SOCl$_2$ is irreversible. In addition, two peaks mean that the reduction is a two-step electron transfer process. Compared with the blank, the maximum reduction current increases markedly in the presence of porphyrin or metalloporphyrins and the highest reduction current emerges by adding CoPp.

Mechanism analysis

The Li/SOCl$_2$ battery consists of a Li anode, a carbon cathode, and the LiAlCl$_4$/SOCl$_2$ electrolyte solution. The electrode reaction of Li/SOCl$_2$ battery is as follows:
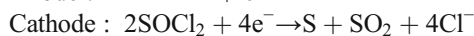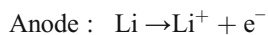
$$\text{Anode}: \quad \text{Li} \rightarrow \text{Li}^+ + e^-$$
$$\text{Cathode}: \quad 2\text{SOCl}_2 + 4e^- \rightarrow \text{S} + \text{SO}_2 + 4\text{Cl}^-$$

Fig. 5 The discharge curves of the Li/SOCl$_2$ battery
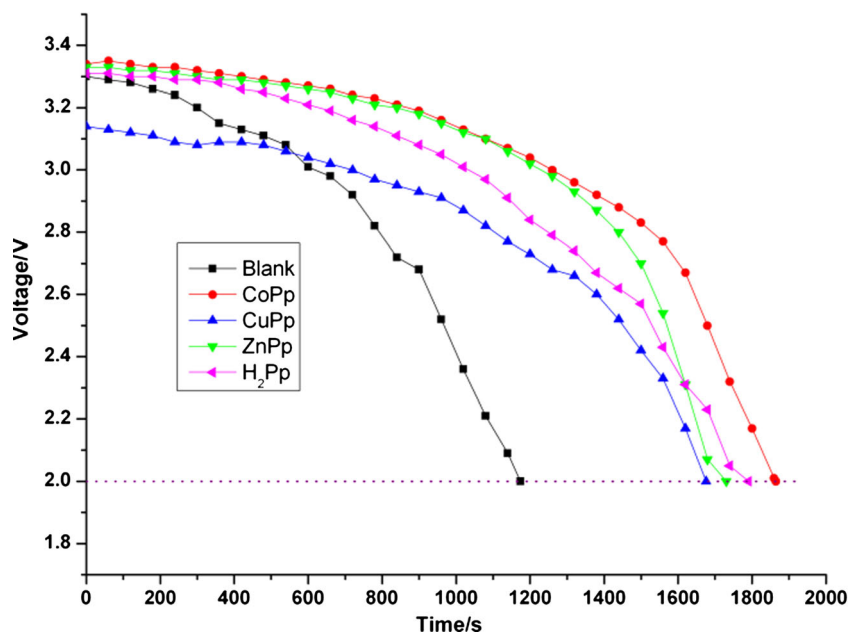
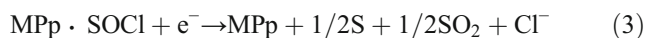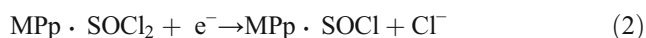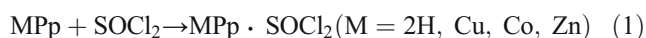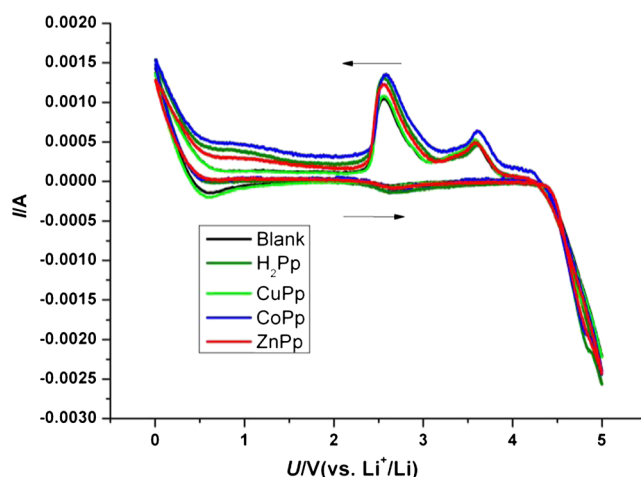**Table 2** The average discharge voltage (U_{av}), discharge time above 2 V (t), energy (E), and capacity (C) of Li/SOCl$_2$ battery

	U_{av} (V)	t (s)	E (J)	C (mA h)
Blank	2.87	1,173.8	96.3	9.3
H$_2$Pp	2.93	1,791.2	153.1	14.5
CuPp	2.83	1,675.8	133.6	13.1
CoPp	3.00	1,865.1	167.2	15.5
ZnPp	3.03	1,730.4	158.3	14.5

Fig. 7 The cyclic voltammetry curves of Li/SOCl$_2$ batteries in the presence of porphyrin or metalloporphyrins

The mechanisms of porphyrins effect on Li/SOCl$_2$ battery have been demonstrated in our previous works [24, 25]. The porphyrins or metalloporphyrins can improve the properties (discharge time, energy, capacity, and maximum initial discharge voltage) of Li/SOCl$_2$ battery from two aspects: one is to increase the reaction rate of SOCl$_2$ reduction due to the coordination to metalloporphyrins and another is to retard the deposition of LiCl crystallite by adding the metal-free porphyrins to the electrolyte.

From the result of cyclic voltammetry, reduction current of Li/SOCl$_2$ battery with porphyrins is higher than that of battery in absence of porphyrins, and higher reduction current is due to higher reaction rate of SOCl$_2$ reduction. In other words, the adding of porphyrins improves the reduction rate of SOCl$_2$. But we do not exclude the possibility that the current enhancement of Li/SOCl$_2$ battery after adding H$_2$Pp is due to retard the deposition of LiCl on cathode.

The mechanism conjectured by the results of experiment includes three steps:

$$MPp + SOCl_2 \rightarrow MPp \cdot SOCl_2 (M = 2H, Cu, Co, Zn) \quad (1)$$

$$MPp \cdot SOCl_2 + e^- \rightarrow MPp \cdot SOCl + Cl^- \quad (2)$$

$$MPp \cdot SOCl + e^- \rightarrow MPp + 1/2S + 1/2SO_2 + Cl^- \quad (3)$$

Firstly, the MPp·SOCl$_2$ adduct which makes SOCl$_2$ active was formed by the interaction of MPp and SOCl$_2$. Afterwards, the MPp·SOCl$_2$ get one electron to produce MPp·SOCl, then S and SO$_2$ are formed when MPp·SOCl get another electron.

In addition, we also found that metalloporphyrins exhibit different improvement to Li/SOCl$_2$ battery, and the Li/SOCl$_2$ battery with CoPp shows the highest energy and capacity. This maybe due to the reason that the Co^{2+} ion is more easily to coordinate with SOCl$_2$ and to be oxidized to Co^{3+} when in the electrolyte, compared with Cu^{2+} and Zn^{2+} ions.

Conclusion

One porphyrin (H$_2$Pp) and three corresponding metalloporphyrins (CuPp, CoPp, ZnPp) have been synthesized, characterized, and used to improve Li/SOCl$_2$ battery performance. The discharge time above 2 V of Li/SOCl$_2$ battery with porphyrins is approximately 502–692 s longer than that of Li/SOCl$_2$ battery in blank. The maximum initial discharge voltage of battery is increased by 0.04 V for CoPp and 0.03 V for ZnPp while that of battery with CuPp decreased. The energy of Li/SOCl$_2$ battery in blank is also increased. The capacity of Li/SOCl$_2$ battery with porphyrins is approximately 40–67 % higher than that of Li/SOCl$_2$ battery in blank. The results show that CoPp exhibits high efficiency to improve Li/SOCl$_2$ battery; therefore, it is worth to do further research on the CoPp. The results of cyclic voltammetry show that the adding of porphyrins improves the reduction rate of SOCl$_2$.

Fig. 6 Energy of Li/SOCl$_2$ battery in presence of porphyrins

References

1. Guidotti RA, Reinhardt FW, Odinek J (2004) J Power Sources 136:257–262
2. Ratnakumar BV, Smart MC, Kindler A, Frank H, Ewell R, Surampudi S (2003) J Power Sources 119:906–910
3. Jain M, Nagasubramanian G, Jungst RG, Weidner JW (1999) J Electrochem Soc 146:4023–4030
4. Gu WB, Wang CY, Weigner JW, Jungst RG, Nagasubramanian GJ (2000) J Electrochem Soc 147:427–434
5. Cho YI, Chee DW (1991) J Electrochem Soc 138:927–930
6. Chung K, Lee JS, Ko YO (2005) J Power Sources 140:376–380
7. Choi YK, Kim WS, Chung K, Chung MW, Nam HP (2000) Microchem J 65:3–15
8. Kim WS, Choi YK (2003) Appl Catal 252:163–172
9. Zhang RL, Wang JF, Xu B, Huang XY, Xu ZW, Zhao JS (2012) J Electrochem Soc 159:704–710
10. Carmier D, Vix-Guterl C, Lahaye J (2001) Carbon 39:2181–2186
11. Carmier D, Vix-Guterl C, Lahaye J (2001) Carbon 39:2187–2193
12. Novák P, Müller K, Santhanam KSV, Haas O (1997) Chem Rev 97:207–281
13. Chen M, Herzel Y (2004) J Power Sources 136:268–275
14. Xu ZW, Zhang GX, Cao ZY, Zhao JS, Li HJ (2010) J Mol Catal 318:101–105
15. Kim WS, Sim WJ, Chung K, Sung YE, Choi YK (2002) J Power Sources 112:76–84
16. Kubat P, Lang K, Janda P, Anzenbacher PJ (2005) Langmuir 21:9714–9720
17. Mitsuhiko M, Kazuya O, Kenji K, Koji O, Yoshiaki K (2010) Chem Commun 46:2121–2123
18. Sun WJ, Li J, Yao GP, Zhang FX, Wang JL (2011) Appl Surf Sci 258:940–945
19. Merlau ML, Del PMM, Nguyen SBT, Hupp JT (2001) Angew Chem Int Ed 40:4239–4242
20. Leonardi MJ, Topka MR, Dinolfo Peter H (2012) Inorg Chem 51:13114–13122
21. Hutchison JE, Postlethwaite TA, Chen CH, Hathcock KW, Ingram RS, Ou W, Linton RW, Murray RW, Tyvoll DA, Chng LL (1997) Langmuir 13:2143–2148
22. Zak J, Yuan HP, Ho M, Woo LK, Porter MD (1993) Langmuir 9:2772–2774
23. Jeong NC, Son HJ, Prasittichai C, Lee CY, Jensen RA, Farha OK, Hupp JT (2012) J Am Chem Soc 134:19820–19827
24. Su XQ, Sun WJ, Li J, Zhang ZQ, Jiang M, Zhao JS (2014) ECS Electrochem Lett 3:A39–A40
25. Su XQ, Li J, Yao GP, Wang JL, Zhao JS, Zhang FX (2013) Catal Commun 37:23–26
26. Baturina OA, Kanevsky LS, Bagotzky VS, Volod'ko VV, Karasev AL, Revina AA (1991) J Power Sources 36:127–136
27. Kim WS, Choi YK, Chjo KH (1994) Bull Korean Chem Soc 15:456–460
28. Wang C, Li J, Mele G, Yang GM, Zhang FX (2007) Appl Catal 76:218–226
29. Yu GF, Zhang XJ, Wang C, Zhang WW, Yang CX (2013) J Electrochem Soc 160:A2027–A2032
30. Zhang YH, Chen DM, He TJ, Liu FC (2003) Spectrochim Acta A 59:87–101
31. Kitagawa T, Ozaki Y (1987) Struct Bond 64:71–114
32. Boucher LJ, Katz JJ (1967) J Am Chem Soc 89:1340–1349